

Electrochemical Quartz Crystal Microbalance (EQCM) Studies of Ions and Solvents Insertion into Highly Porous Activated Carbons

Mikhael D. Levi,[†] Naomi Levy,[†] Sergey Sigalov,[†] Gregory Salitra,[†] Doron Aurbach,^{*,†} and Joachim Maier[‡]

Department of Chemistry, Bar-Ilan University, Ramat-Gan 52900, Israel, and Max Planck Institute for Solid State Research, Heisenbergstr. 1, 70569 Stuttgart, Germany

Received June 2, 2010; E-mail: aurbach@mail.biu.ac.il

Abstract: Electrochemical quartz crystal microbalance (EQCM) technique provides a direct assessment to the behavior of electroadsorbed ions and solvent molecules confined in micropores of activated carbon electrodes in contact with practically important aprotic electrolyte solutions. The estimated value of the solvation number equal to 3 is evident for a partial desolvation of Li^+ cations when adsorbed in carbon micropores.

Highly microporous activated carbons (ACs) are attractive practical materials used in high power energy storage devices (supercapacitors),¹ capacitive deionization of nonpotable water (desalination),² nontraditional production of renewable electric energy based on the difference in water salinity,³ and more. The common feature of these devices and technologies is the ability of the ACs to store electric charge reversibly within the electric double layer (EDL), composed of electronically charged carbon pores walls counterbalanced by layers of oppositely charged, electrostatically adsorbed ions, transported from the electrolyte solution into the pores. While a major effort has been made to understand the relation between the pore/ion size ratio and the specific capacitance of carbon electrodes,^{4–6} less attention has been paid to their kinetic behavior, studied commonly by conventional electroanalytical techniques (voltammetry, electrochemical impedance spectroscopy, etc). It was recently demonstrated⁷ that thin composite carbon electrodes in electrochemical quartz crystal microbalance (EQCM) measurements demonstrate a clear gravimetric response that enables the sensitive probing of compositional changes in the electrodes' microporous structure during their charging under a wide variety of dynamic conditions.

The goal of this communication is to demonstrate the unique ability of the EQCM to reflect such compositional changes in microporous ACs in contact with important nonaqueous systems such as propylene carbonate (PC) solutions of quaternary (tetraalkyl) ammonium salts, $(\text{TAA})\text{BF}_4$, where TAA denotes tetra-ethyl, -butyl, and -octylammonium cations (TEA^+ , TBA^+ and TOA^+ , respectively). The EQCM responses obtained using moderately solvated TEA^+ ,⁸ slightly solvated, bulkier TBA^+ and TOA^+ cations with degraded pore size commensurability, and, finally, highly solvated Li^+ cations⁹ provide important fingerprints of the adsorbed ions and solvent molecules, confined in nanometer size pores of the AC electrodes upon their charging. Facile decomposition (desolvation) of adsorbing $\text{Li}^+(\text{PC})_x$ solvo-complexes allows for the direct assessment of the confined ion solvation number. The result obtained corroborates well with the recent quantum-chemical

characterization of the same solvo-complexes based on the density functional theory (DFT).¹⁰

In order to reach the above goal, a typical microporous AC YP-17 (Kuraray, Japan) was chosen with a BET surface area of $1600 \text{ m}^2\text{g}^{-1}$ and an average particle size of around a few micrometers (for other structural details and the technique of coating the crystal with a carbon slurry, see Supporting Information, sections 1 and 2). Note that the carbon micropores with their width $d < 2 \text{ nm}$ account for about 87% of the total pore volume (Figure S1C), and 55% of the total pore volume relates to the micropores narrower than 1.2 nm. Thus, a large number of carbon micropores are inaccessible to TOA^+ cations (the diameter is 1.12 nm) but are perfectly permeable for the smaller TEA^+ cations (the diameter is 0.68 nm; see Table S1 and Figure S1C).

Cyclic voltammetric curves (CVs) of carbon electrodes obtained simultaneously with their EQCM responses for three different $(\text{TAA})\text{BF}_4$ salts (Figure 1A) show a spectacular ion-sieving effect⁶ as the size of the cation increases. The bulky TOA^+ cations resulted in a 55% decrease in the reversible charge at the negatively charged carbon surface, compared to that for the much smaller TEA^+ cations. Note that the smallest Li^+ cation (0.152 nm, see Table S1), which is highly solvated in PC, shows practically the same reversible charge as that obtained with the TEA^+ cation (Figure 1B).

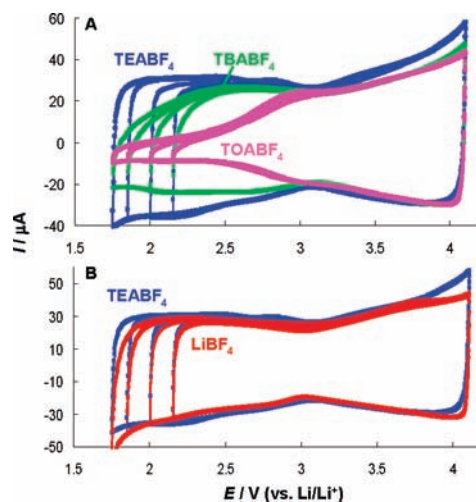


Figure 1. CVs of a carbon-coated quartz crystal electrode in 0.1 M TEABF_4 , TBABF_4 , TOABF_4 , LiBF_4 solutions in propylene carbonate (PC) as indicated. Scan rate 20 mV s^{-1} .

TEABF_4 was selected for a detailed CV and EQCM characterization of the AC electrodes as a function of the supporting electrolyte concentration. Figure 2A shows the related CVs with a

[†] Bar-Ilan University.

[‡] Max Planck Institute for Solid State Research.

characteristic V-shaped minima, sharpening with dilution of the electrolyte solution, and accompanied by mass changes of the carbon electrode due to adsorption/desorption of the ions (Figure S3). From a simple electrostatic consideration, these are believed to be anions or cations, as the potential is swept positively or negatively, respectively, from the potential of zero charge (*pzc*). In order to quantitatively correlate the mass changes of the adsorbed ions and solvent molecules with the potential-induced variation of the electrode charge density, one should know at least one reference point on each axis (potential and mass change): (i) the potential of zero charge (evaluated as 3.08 V versus Li/Li⁺ by three independent methods; see Figure S4) and (ii) the so-called potential of zero mass change (*pzmc*) that separates the mass changes of the electrode due to adsorbed anions and cations (Figure S4 and Table S1). Owing to the essentially broad minimum in the mass change curves at small charge densities, the *pzmc* can be ascribed to the *pzc*, thus simplifying the assessment of the mass of the adsorbed ions versus charge density. Prior to quantifying the EQCM responses under consideration, we verified that the scan rate below 50 mV s⁻¹ prevented the mass versus potential curves from undesirable kinetic limitations of charging the AC electrode (Figure S5).

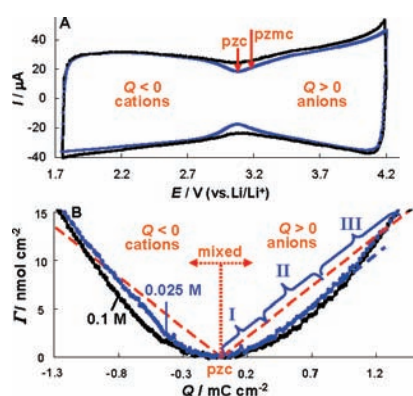


Figure 2. CVs of a carbon-coated quartz crystal electrode in 0.1 and 0.025 M TEABF₄/PC solutions (A), and the related treated EQCM responses, Γ vs Q (B). Three domains with the characteristic different Γ/Q slopes for the 0.025 M solution are indicated. The slope within domain II (the broken blue line) is equal to the theoretical slope of the broken red straight line calculated from the Faraday law. The different values of the slopes of the Γ versus Q plot within domains I–III are discussed in detail in the main text.

It is advantageous to present the total mass changes due to adsorbed ions and solvent (μg per 1 cm² of piezoactive area of the crystal) and their individual contributions by the changes of the amounts of these species (i.e., their population), Γ , expressed in nmol cm⁻². The values of Γ appearing in the curves of Figure 2B were thus obtained by dividing the experimental mass change of the electrode due to adsorption of anions and cations (at $Q > 0$ and $Q < 0$, respectively) by the molar masses of the unsolvated ions. The method allowing for such a separation was adapted from the approach used to separate ion and solvent fluxes in doped conducting polymers.¹¹ Figure 2B shows the plots of Γ versus charge density for two different concentrations of TEABF₄, corresponding to the CVs shown in Figure 2A. The theoretical changes of the amount of the adsorbed cations and anions, calculated from the Faraday law, are shown for comparison as the two red broken straight lines (Figure 2B), originating from $Q = 0$, with equal absolute values of their slopes (since we used a symmetrical 1:1 TEABF₄ salt). A quantitative analysis is further performed for the positively charged carbon surface (adsorption of anions, which are poorly solvated in aprotic solutions as compared

to small, highly solvated Li⁺ cations).¹² It should be emphasized that this type of plot, Γ versus Q , is quite typical for the slightly solvated (bulky) ions, as was earlier reported for the adsorption of Cs⁺ cations on the AC in aqueous solutions.⁷

Within domain I (near the *pzc*, 0.025 M TEABF₄/PC solution, the electrode charge densities $Q < 0.26$ mC cm⁻²) the experimental curve has a shallow minimum, attributed to a cation–anion mixing due to a breakdown of perm-selectivity in AC micropores (adsorption of counterions, here BF₄⁻ anions, is accompanied by desorption of the related co-ions, i.e. TEA⁺ cations). On the one hand, this conclusion is in agreement with the narrower minimum on the Γ versus Q plot for the more dilute solution as compared to the concentrated one (Figure 2B), and on the other hand, it is fully consistent with the view of ions and solvent molecules, confined in carbon micropores, obtained by molecular dynamics (MD) simulations.^{13,14} At intermediate charge densities (domain II), the slope of the experimental Γ versus Q plot ($0.26 < Q < 0.90$ mC cm⁻², $R^2 = 0.991$; see the broken blue line in Figure 2B) becomes equal to the theoretical slope (the broken red line). Finally, the slope increases to the point that the experimental Γ versus Q curve crosses the theoretical straight line at the limit of high electrode charge densities (domain III, $Q > 0.90$ mC cm⁻²).

In order to describe the increase in the Γ/Q ratio with electrode charge density, we propose several plausible scenarios of the potential-dependent dimensional changes in porous AC electrodes. Within domain I, the total porous volume in microporous carbons may be conserved, since in place of the excluded (desorbed) co-ions the counterions enter the pore (adsorb). Recent MD studies not only confirm partitioning of both the counterion and co-ions in nanometer size pores of ACs¹⁴ but also predict a distinct ordering (densification) of the PC molecules adsorbed in carbon micropores once the TEABF₄ salt is introduced into PC solvent.¹³

The theoretical Γ/Q ratio observed typically within domain II implies that as the charge density increases, the ions enter the accessible pores' volume effectively without their solvation shells. The energy cost of stripping the BF₄⁻ ions from the solvated PC molecules is surprisingly small (ten times smaller than for the Li⁺(PC)₄).¹² However, in order to be adsorbed, the anions still need some free space in carbon micropores. This can be ensured by a charge-induced expansion of the carbon micropores due to the elongation of the C–C bonds (proved, e.g., for carbon nanotubes^{15,16}). Moreover, the increase in length of the activated porous carbon sample upon increasing charge density, closely resembling the classical electrocapillary effect, has been discovered long ago, using Moiré deflectometry.¹⁷ Finally, within domain III, the high Γ/Q ratio may be caused by the high extent of elongation of the C–C bonds, resulting in distortion of the carbon hexagonal rings with increasing charge density,¹⁶ and/or implies a strong, charge density induced deformation of the carbon micropores, originated from the interplay between the increased electrostatic and volume exclusion interactions.¹⁴ Since the population of ions in microporous ACs is controlled by the electrode charge density, the increasing deformation of carbon micropores leads to their expansion, allowing an additional amount of solvent molecules to enter the carbon micropores thus effectively increasing the resulting Γ/Q ratio as compared to the theoretical one.

In contrast to anions, which are only slightly solvated in aprotic solvent solutions, the much stronger solvated Li⁺ cations¹² tend to bring a part of their solvation shell at a surprisingly low charge density with the concomitant raise in its Γ/Q ratio as compared to the theoretical one (Figure 3). The Γ versus Q plots for the carbon electrode measured in 0.05 and 0.10 M LiBF₄/PC solutions demonstrate a clear reduction of the Γ (total = ions + solvent) for

a more concentrated solution (Figure S6), implying a better screening (i.e., a shorter Debye length) of the long-range electrostatic repulsion between heavily charged walls of AC micropores, which is expected to effectively decrease the pore deformation (expansion).¹⁴

Figure 3 demonstrates clearly a gradual increase in confinement of the cations in the accessible AC micropores in the sequence: $\text{Li}^+ < \text{TEA}^+ < \text{TBA}^+ < \text{TOA}^+$ resulting in a peculiar coupling (in this series) of a diminishing solvation ability of the cations with the increasing tendency for breaking down the carbon pores permselectivity. Looking closely at the respective slopes of the Γ (total) versus Q plots, one can note that the flattening of the major portion of the cathodic Γ versus Q curve with the increasing size of the cation (and, hence decreasing the accessible microporous volume of the activated carbon, Figure S1B) can be regarded as the extension of the lower Γ/Q ratio near the pzc toward higher negative charge densities. This implies that the bulkier cations are less effective (as the counterions) in keeping the electroneutrality in the carbon pores during their charging, forcing the smaller (and hence more mobile) co-ions to play an increasing role in the charge compensation mechanism (compare with the likely mechanism in electroactive polymers).¹⁸

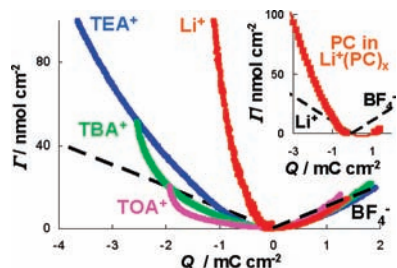


Figure 3. Amount of cations and anions, Γ , adsorbed at negatively and positively charged carbon surface, respectively, as a function of the charge density, Q , for the different salts dissolved in PC, which were measured in parallel to the CVs shown in Figure 1. The theoretical Γ versus Q plots (the broken black straight lines) were calculated on the basis of the Faraday law. The inset compares the amount of solvent molecules (the solid red curve), accompanying adsorption of the Li^+ cations (the left broken black line). Their ratio is close to 3, confirming the partial desolvation of Li^+ cations confined in carbon micropores.

It is instructive to emphasize the outstanding ability of the EQCM measurements to reveal coadsorption of solvent molecules, accompanying adsorption of highly solvated cations. Li^+ cations form stable solvo-complexes with four PC molecules^{9,10,12} (considered as a primary solvation shell) with an average diameter of 1.19 nm,⁹ which is close to the size of the unsolvated TOA^+ cation, 1.12 nm (Table S1). The confinement of these cations in the microporous carbon appears to be drastically different. The TOA^+ cations are much less polarizable and, hence, less adjustable for the confinement in the subnanometer size carbon pores compared to the more flexible $\text{Li}^+(\text{PC})_4$ solvo-complexes.¹⁰ A recent MD study of the family of $\text{Li}^+(\text{PC})_x$ solvo-complexes has clearly demonstrated a remarkable adjustment of the PC molecules to varying concentrations of Li salt irrespective of the space confinement,¹⁴ which is believed to

be one of the major contributions to the enhanced differential capacitance in subnanometer size carbon pores.⁴

The insert in Figure 3 compares the amount of PC molecules (the solid red curve), accompanying the adsorption of Li^+ cations (the left broken black line). Their ratio is close to 3, confirming a partial desolvation of the Li^+ cations, confined in carbon micropores.¹⁰

In summary, we demonstrated herein the unique ability of EQCM measurements to provide a direct assessment to the solvation number of Li^+ cations, confined in AC micropores, and to reflect the enhanced breakdown of perm-selective behavior in carbon micropores in the presence of the bulky quaternary ammonium cations, extended toward higher negative charge densities of the carbon surface. These are new features of EDL structure in microporous AC carbons, demonstrated for both slightly and highly solvated ions, which appear to be in good agreement with recent molecular dynamic studies of highly porous carbons and carbon nanotubes. Applying the EQCM, we envisage further important breakthroughs in our understanding of charging mechanisms in microporous electrodes and the dynamics of ions and solvent molecule transport phenomena.

Acknowledgment. A partial support for this work was obtained by the GIF (German-Israel Foundation) and the Ministry of Absorption (Israel).

Supporting Information Available: Additional experimental details and characterization of pristine carbon powder. This material is available free of charge via the Internet at <http://pubs.acs.org>.

References

- (1) (a) Kotz, R.; Carlen, M. *Electrochim. Acta* **2000**, *54*, 2483. (b) Simon, P.; Gogotsi, Y. *Nat. Mater.* **2008**, *7*, 845.
- (2) (a) Avraham, E.; Bouhadana, Y.; Soffer, A.; Aurbach, D. *J. Electrochem. Soc.* **2009**, *156*, 95. (b) Biesheuvel, P. M.; Bazant, M. Z. *Phys. Rev. E* **2010**, *81*, 031502–03.
- (3) Brogioli, D. *Phys. Rev. Lett.* **2009**, *103*, 058501.
- (4) Chmiola, J.; Yushin, G.; Gogotsi, Y.; Portet, C.; Simon, P.; Taberna, L. *Science* **2006**, *313*, 1760.
- (5) (a) Largeot, C.; Portet, C.; Chmiola, J.; Taberna, P.-L.; Gogotsi, Y.; Simon, P. *J. Am. Chem. Soc.* **2008**, *130*, 2730. (b) Fernandez, J. A.; Arulepp, M.; Leis, J.; Stoeckli, F.; Centeno, T. A. *Electrochim. Acta* **2008**, *53*, 7111.
- (6) (a) Lin, R.; Taberna, P. L.; Chmiola, J.; Guay, D.; Gogotsi, Y.; Simon, P. *J. Electrochem. Soc.* **2009**, *156*, A7. (b) Eliad, L.; Salitra, G.; Soffer, A.; Aurbach, D. *J. Phys. Chem. B* **2001**, *105*, 6880.
- (7) Levi, M. D.; Salitra, G.; Levy, N.; Aurbach, D.; Maier, J. *Nat. Mater.* **2009**, *8*, 872.
- (8) Yang, C.-M.; Kim, Y.-J.; Endo, M.; Kanoh, H.; Yudasaka, M.; Iijima, S.; Kaneko, K. *J. Am. Chem. Soc.* **2007**, *129*, 20.
- (9) Endo, M.; Maeda, T.; Takeda, T.; Kim, Y. J.; Koshihara, K.; Hara, H.; Dresselhaus, M. S. *J. Electrochem. Soc.* **2001**, *148*, A910.
- (10) Ohtani, H.; Hirao, Y.; Ito, A.; Tanaka, K.; Hatozaki, O. *J. Therm. Anal. Calorim.* **2010**, *99*, 139.
- (11) Hillman, A. R.; Daisley, S. J.; Bruckenstein, S. *Electrochim. Acta* **2008**, *53*, 3763.
- (12) Soetens, J.-C.; Millot, C.; Maignet, B. *J. Phys. Chem. A* **1998**, *102*, 1055.
- (13) Tanaka, A.; Iiyama, T.; Ohba, T.; Ozeki, S.; Urita, K.; Fujimori, T.; Kanoh, H.; Kaneko, K. *J. Am. Chem. Soc.* **2010**, *132*, 2112.
- (14) Kiyohara, K.; Sugino, T.; Asaka, K. *J. Chem. Phys.* **2010**, *132*, 144705.
- (15) Li, C.-Y.; Chou, T.-W. *Nanotechnology* **2006**, *17*, 4624.
- (16) Guo, W.; Guo, Y. *Phys. Rev. Lett.* **2003**, *91*, 115501.
- (17) Oren, Y.; Glatt, I.; Livnat, A.; Kafri, O.; Soffer, A. *J. Electroanal. Chem.* **1985**, *18*, 7–59.
- (18) (a) Hillman, A. R.; Mohamoud, M. A.; Bruckenstein, S. *Electroanalysis* **2005**, *17*, 1421. (b) Bruckenstein, S.; Brzezinska, K.; Hillman, A. R. *Phys. Chem. Chem. Phys.* **2000**, *2*, 122.

JA104391G